DEPENDENCY OF EQUIVALENCE RATIO ON HYDROGEN CYLINDRICAL DETONATION INDUCED BY DIRECT INITIATION

Asahara, M.[1], Tsuboi, N.[2] Hayashi, A.K.[3] and Yamada, E.[4]
[1] Department of Mechanical Engineering, Aoyama Gakuin University, 5-10-1 Fuchinobe, Chuo, Sagamihara, Kanagawa, 252-5258, Japan, asahara@flab.isas.jaxa
[2] Department of Mechanical and Control Engineering, Kyushu Institute of Technology,1-1 Sensui, Tobata, Kitakyushu, Fukuoka, 804-8550, Japan, tsuboi@mech.kyutech.ac.jp
[2] Department of Mechanical Engineering, Aoyama Gakuin University, 5-10-1 Fuchinobe, Chuo, Sagamihara, Kanagawa, 252-5258, Japan, hayashi@me.aoyama.ac.jp
[3] Department of Mechanical Engineering, Aoyama Gakuin University, 5-10-1 Fuchinobe, Chuo, Sagamihara, Kanagawa, 252-5258, Japan, yamada@me.aoyama.ac.jp

Abstract

A hydrogen fuel is expected to expand its demand in the future. However, hydrogen has to be treated with enough caution because of wide combustible conditions and easiness to ignite. Detonation accidents are caused in hydrogen gas such as the explosion accident in Fukushima first nuclear plant (2011). Therefore, it is necessary to comprehend initiation conditions of detonation to prevent its detonation explosion. In the present study, cylindrical detonation induced by direct initiation is simulated to understand the dependency of equivalence ratios in hydrogen-oxygen mixture. The several detailed kinetic models are compared to select the most appropriate model for detonation in a wide range of equivalence ratios. The Petersen-Hanson model is used in the present study due to the best agreement among the other models. In the numerical results of cylindrical detonation induced by direct initiation, a cellular structure, which is similar to the experimental smoked foil record, is observed. The local pressure is up to 12 MPa under the condition at the standard state. The ignition process of cylindrical detonation has two stages. At the first stage, the normalized cell width, $\lambda/L_{1/2}$, at each equivalence ratio increases linearly. At the second stage, cell bifurcations appear due to a generation of new transverse waves. It is observed that a transverse wave transforms to a transverse detonation at the end of the first stage, and after that, some disturbance is developed to be a new transverse wave at the beginning of the second stage.

1.0 INTRODUCTION

Hydrogen fuel is paid attention to solve the energy problem which presently relies heavily on fossil fuel. Hydrogen is carbon free and clean fuel. Therefore it is expected to expand its consumption for the future. However, hydrogen must be treated with a full caution due to its inflammability and easy ignitability. Many hydrogen explosion accidents occur in hydrogen storage tank and hydrogen leak in chemical plants. The recent Fukushima first nuclear plant accident [1] is related with the hydrogen explosion, where hydrogen might be produced by water radiolysis under high pressure and high temperature, or by zirconium reaction. The pipe was exploded through hydrogen detonation in the Hamaoka nuclear plant in 200l [2]. Despite explosion hazard, these accidents are totally detonation which pressure becomes more than thousand atmospheres [3] and deflagration-to-detonation (DDT) occurs there. Detonation is a supersonic combustion wave propagating with a leading shock wave followed by a flame in reactive mixture. In the high pressure and high temperature condition, the reaction accelerates through the shock waves interaction together with a large heat release in a short time. Such detonation accidents cause the enormous damages, and then detonation initiation must be elucidated for the engineering safety.

Detonation initiation is classified by two processes: one is a direct initiation and another is an indirect initiation. Direct initiation of detonation occurs mainly by charging a high enough energy source to a detonable gas mixture. The direct initiation of detonation may need more energy and may occur with much difficulty. The indirect initiation occurs through DDT. Many experimental studies [4-6] have been performed for DDT to elucidate its detonation initiation conditions. The cylindrical or spherical

detonation initiated directly propagates from a point source to the surrounding. Many previous experimental works using direct initiation were performed using hydrocarbon fuels. However, hydrocarbon fuel detonation will also provide worthy information to study hydrogen-oxygen detonation. Zel'dovich et al. [6] first reported the experimental study of expanding detonation. They formulated, experimentally and theoretically through the blast wave theory, the relation between the blast wave and the characteristic reaction time to indicate the existence of minimum energy (critical energy) for initiation. Bach et al. [7,8] experimentally investigated the critical energy in an acetylene-oxygen system to show that the direct initiation needs the higher energy than the theoretical one obtained by Zel'dovich et al. [6]. Bach et al. classified the initiation process by three regimes; supercritical, critical, and subcritical regime, using a relation between the source energy, E_s, and the critical energy, E_c. As the source energy is higher than the critical energy ($E_s > E_c$), the expanding detonation initiates directly due to the high energy release (the supercritical regime). As the source energy is the almost same as the critical energy ($E_s \approx E_c$), detonation propagates in a special manner that the reaction region decoupled about 3mm from a shock wave in such a so-called quasi-steady state [9,10]. Then the local explosion occurs at a point behind the shock wave and it spreads along a tangential direction to the propagating direction of detonation front (the critical regime). As the source energy is lower than the critical energy ($E_s < E_c$), the reaction front decouples from the shock front to decelerate the expanding shock wave (the subcritical regime). Lee et al. [9-13] revised the theory by Zel'dovich et al. to propose a theory to predict the critical energy. The equation through this theory is obtained from the initial pressure, Chapman-Jouguet Mach number, and cell size to explain the quasi-steady detonation in term of the critical energy [13]. The theory by Lee et al. has developed for acetylene-oxygen system but can be used for hydrogen-oxygen system [14,15]. However, in spite of the many previous studies, there are few experimental data of the direct initiation with the hydrogen-oxygen mixture without dilution.

In order to solve this direct initiation problem, hydrogen-oxygen system is simulated by He and Clavin [16] to perform one-dimensional theoretical model of a point blast direct initiation. He [17] later obtained the critical energy using the critical radius, R_c, and critical velocity, D_c. When the activation energy is small (stable detonation), the shock wave propagates more than the critical velocity, D_c, to reach the critical radius, R_c, then the detonation initiates. When the activation energy is large (unstable detonation), the detonation does not initiate regardless of the relation between the critical radius, R_c, and the critical velocity, D_c. Eckett et al. [18] showed that the unsteadiness of the induction zone is dominant for the failure of expanding detonation. Ng et al. showed the correlation of the critical energy with an induction zone length [19] to explain the various dependencies among the critical conditions using the semi-empirical models in hydrogen-air mixture [20,21]. They performed one-dimensional simulation for the direct initiation of spherical detonation to predict the critical energy and to fit their results with the experimental ones. However, in order to get more accurate results, the multi-dimensional approach is necessary for the simulation of the unstable quasi-state detonation and the dynamics of expanding detonation by the direct initiation. The two-dimensional simulation of the direct initiation was examined by Watt and Shape [22], Nirasawa and Matsuo [23] and Asahara et al. [24]. They showed the cell structure and unsteadiness of the expanding detonation. Jiang et al. [25] obtained the cell bifurcation which is the characteristic phenomena of the expanding detonation and classified the bifurcating process into four modes. These studies are revealing the characteristic of the expanding detonation wave induced by the direct initiation, but the further investigations are necessary to comprehend it. Almost all of the present two-dimensional simulations on expanding detonation by direct initiation were performed in an initial condition. We notice the effect of the initial condition (especially equivalence ratio) on the detonation initiation, which involves compensating for luck of experimental information about the direct initiation in the hydrogen-oxygen mixture.

The main purpose of the present study is to investigate the propagation mechanism of the expanding detonation induced by the direct initiation and to obtain the effect of the equivalence ratio on the detonation initiation and propagation process. Here we perform two-dimensional simulation of cylindrical detonation by the direct initiation at the different equivalence ratio. In order to simulate it, the proper detailed chemical kinetics model is examined to compare the some prospective models.

2.0 CHAPMAN-JOUGUET VALUES FOR SAFETY INDEX

Although detonation has three-dimensional structure, Chapman-Jouguet (CJ) theory, which is obtained by a steady one-dimensional solution, predicts properties of actual detonation reasonably. In this section, we describe the information of CJ values in order to comprehend characteristics of hydrogen-oxygen mixture. Figure 1 shows the relation between equivalence ratio and velocity, pressure, Mach number, and temperature of CJ detonation at the initial pressure, P_0 = 0.1, 0.5, 1.0, 5.0, 10.0, 40.0 atm, and the initial temperature, T_0 = 298.15 K, calculated using AISTJAN [26]. The CJ velocity becomes faster at the low equivalence ratio and gently with increasing the equivalence ratio. The CJ pressure profile has a horseshoe-shape curve. It has a local maximum value of 1.91 MPa at ϕ = 1.1. The CJ temperature has the similar profile to the CJ pressure and has a local maximum value of 3683 K at ϕ = 1.0. Table 1 shows CJ velocity, CJ Mach number, CJ pressure and CJ temperature with hydrogen-oxygen mixture at ϕ = 1.0. It indicates that a stoichiometric condition of hydrogen-oxygen at a standard state may create a significant hazard by the detonation accident.

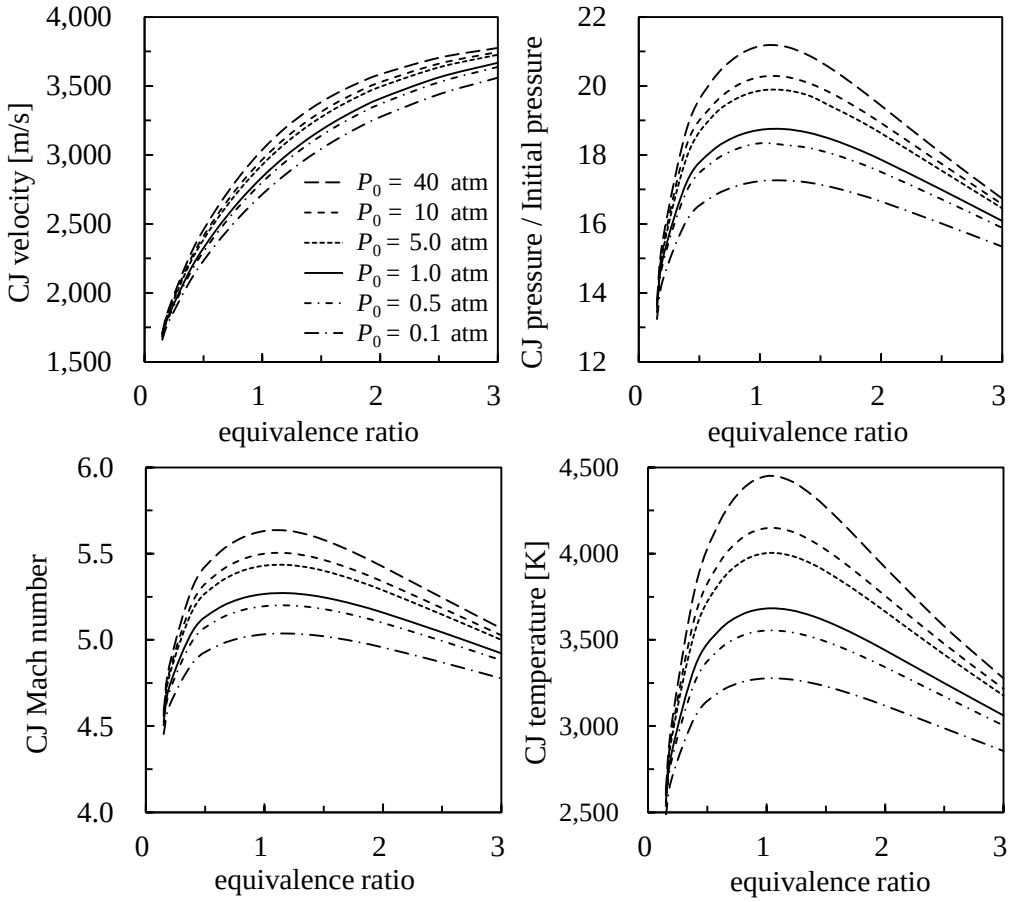

Figure 1. The velocity, pressure, Mach number, and temperature profiles of CJ detonation with hydrogen-oxygen at P_0 = 0.1, 0.5, 1.0, 5.0, 10.0, 40.0 atm and T_0 = 298.15 K calculated with AISTJAN [26].

Table 1. CJ values with a stoichiometric mixture of hydrogen-oxygen (ϕ = 1.0) at a standard state calculated with AISTJAN [26].

CJ velocity, D_{CJ}	2841.6 m/s
CJ Mach number, M_{CJ}	5.28
CJ pressure, P_{CJ}	1.91 MPa
CJ temperature, T_{CJ}	3682.7 K

3.0 COMPARISON OF DETAILED KINETIC MODELS

A detailed kinetic model is composed of many elementary reactions, where all elementary reactions are not necessary. Thus, a proper kinetic model is picked-up by understanding the feature of each model. The kinetic model for detonation must be solved at high pressure condition as discussed in chapter 2.0. Note that the chemical reaction occurs by chemical species (atom-atom, atom-molecular, and molecular-molecular) collision, however, three-body collisions are important at high pressure condition. In this sense, reaction-rate constant has a pressure dependence defined by Lindemann equation at high pressure. Therefore, several detailed kinetic models are compared to pick up the most appropriate model for detonation in a wide range of equivalence ratios. The detailed kinetic models picked-up are shown in Table 2; Nagoya model [28], Petersen-Hanson model [29], Princeton model [30], Lawrence Livemore National Laboratory (LLNL) model [31], Notre Dame model [32], Brussel model [33] and UT-JAXA model [34]. Each model contains eight species; H_2, O_2, O, H, OH, HO_2, H_2O_2 and H_2O. Nagoya model developed by Hishida and Hayashi is improved from Baulch et al.'s model [35] at the temperature range between 900 K and 2500 K. Petersen-Hanson model is based on the hydrogen-oxygen submechanism from the methane-oxidation mechanism of the RAMEC-Gas Research Institute GRI-Mech 1.2. The feature of this model is that the pressure dependence on a forward reaction coefficient includes the third body reactions for H_2O_2 decomposition and recombination. Tsuboi et al. [36,37] showed that the detonation cell size of this model becomes larger than that of the other models such as Nagoya model. Princeton model and LLNL model are similar to each other and are validated by the experimental results of induction time and laminar flame velocity at the wide range of reaction conditions. Brussel model is validated at the wider rage than Princeton model and LLNL model, and is fitted into the experimental data at high pressure conditions. Burke et al. [38] say that the difference between the predicted values by the kinetic model and the experimental values is due to the HO_2-H and HO_2-OH reactions. Shimizu et al. noticed these reactions and proposed UT-JAXA model based on Brussel model. The pressure dependency among the detailed kinetic models is studied by Tsuboi et al., [39] Adachi et al, [40] and Strohle and Myhrvold [41], however, the dependence of equivalence ratio on kinetic model cannot be estimated explicitly.

Table 2. The detailed kinetic models compared the dependency of equivalence ratio.

Model	Number of species, N	Number of elementary reactions, K	Reference
Nagoya	8	19	Hishida and Hayashi, 1991 [28]
Petersen- Hanson	8	18	Petersen and Hanson, 1999 [29]
Princeton	8	19	Li, Zhao, Kazakov and Dryer, 2004 [30]
LLNL	8	19	Conaire, Curran, Simmie, Pitz and Westbrook, 2004 [31]
Notre Dame	8	19	Powers and Paolucci, 2005 [32]
Brussel	8	21	Konnov, 2007 [33]
UT-JAXA	8	21	Shimizu, Hibi, Koshi, Morii and Tsuboi, 2011 [34]

The detonation cell size measured experimentally may be correlated with a variable corresponding to a reaction property of the system such as the initial pressure and the initial equivalence ratio. It is considered that the cell size is a space dimension of the reaction property indetonable gas mixture. On the other hand, the reaction zone width is proposed as the space dimension by the ZND model. Both the cell size and the reaction zone width are the same space dimension parameter. Shchelkin and Troshin [42] reported the linear relation between the cell width and the reaction zone width. Additionally, Knystautas et al. [43] , Westbrook [44], Bull et al. [45], Shepherd [46] and Stamps et al. [47] showed the relation between the cell size and the reaction zone length at the wide range of initial conditions. Thus, the detailed kinetic model can be validated by comparing the reaction zone width based on the detailed kinetic model with the cell size measured experimentally.

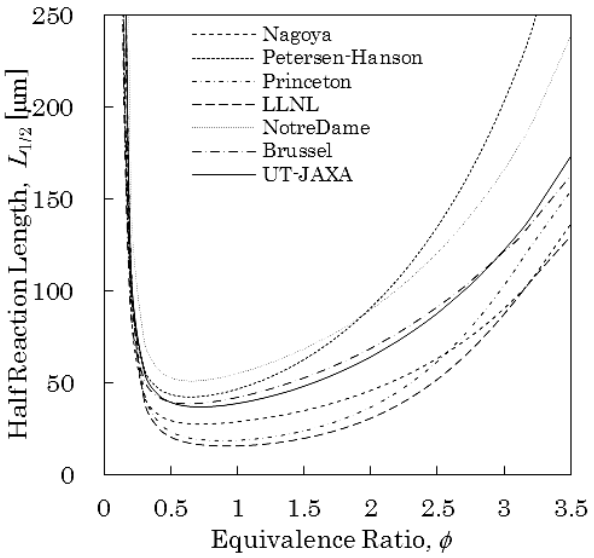

Figure 2. The relation between the equivalence ratio and the half reaction length of each detailed kinetic model at a standard state (P_0 = 1.0 atm, T_0 = 298.15 K) calculated with ZND [49].

In the present study, the half reaction length is used as the characteristic reaction zone width. The half reaction length, $L_{1/2}$, is defined as the distance from the shock wave to the place where the hydrogen mass fraction is equal to the average value between the free stream and the equilibrium steady state [48]. The half reaction length, $L_{1/2}$, is calculated with ZND [49]. Figure 2 shows the relation between the equivalence ratio and the half reaction length for the detailed kinetic models in hydrogen-oxygen mixture at a standard state. The profiles of half reaction lengths become the U-shaped curves shown in Fig. 2. In the previous study [36], the cell size of numerical detonation becomes larger with increasing the half reaction length. It appears that the cell size by Notre Dame model is the largest one at the stoichiometric condition. Figure 3 shows a comparison among the experimental cell width by Ohyagi et al. [50] and the predicted cell widths, λ, by the half reaction length, $L_{1/2}$, given by

$$\lambda = \mathrm{A}L_{1/2}, \tag{19}$$

where A– the proportional constant. For the predicted cell width by Eq. 19, each proportional constant which is obtained as the minimum predicted cell width given by Eq. 19, is equal to the minimum cell width by the experiment. The experimental cell width becomes a minimum at ϕ = 0.7. The proportional constants have the value as shown in Table 3. The curve of Petersen-Hanson model shows the better prediction at a large equivalence ratio than that of others. Therefore, Petersen-Hanson model is selected to study on the dependence of equivalence ratio at direct initiation.

Table 3. The half reaction length, the induction length, and the proportional constant in Fig. 2 using the detailed kinetic models.

Model	$L_{1/2}$ [μm]		L_{ind} [μm]		$L_{1/2,\mathrm{Min}}$ [μm] (equivalence ratio)	A
	ϕ = 0.7	ϕ = 1.0	ϕ = 0.7	ϕ = 1.0		
Nagoya	27.6	28.9	27.0	28.6	27.6 (ϕ = 0.7)	36.1
Petersen- Hanson	42.4	46.6	42.7	46.7	42.4 (ϕ = 0.6)	23.5
Princeton	19.3	18.8	18.1	17.7	18.6 (ϕ = 0.9)	53.7
LLNL	16.6	15.8	15.8	15.2	16.1 (ϕ = 1.1)	63.6
Notre Dame	51.1	55.1	50.1	54.3	51.1 (ϕ = 0.7)	19.5
Brussel	38.9	42.1	39.4	43.1	38.8 (ϕ = 0.6)	25.7
UT-JAXA	36.9	38.8	38.2	40.7	36.9 (ϕ = 0.7)	27.0

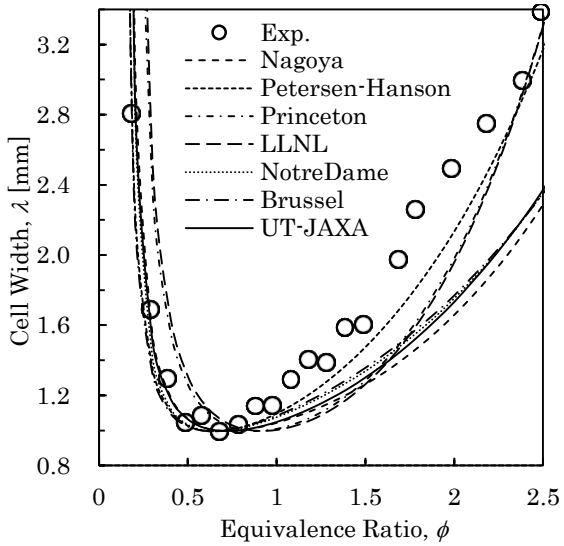

Figure 3. The experimental cell width [50] and the predicted cell width given by the half reaction length in hydrogen-oxygen mixture at a standard state with several equivalence ratios.

4.0 NUMERICAL METHOD

The reaction source terms are treated in a point-implicit manner in order to avoid a stiff problem. Then the second-order MUSCL type AUSMDV scheme [51,52] is used to investigate the scheme dependence in inviscid term. The Shuen's limiter [53] is used as a numerical flux limitation. As discussed in section 3, Petersen-Hanson model [29] is used as the detailed chemical kinetics mechanism to solve with different equivalence ratios. The viscous effects in the present simulation such as turbulence and boundary layer interactions are neglected. Local vortices or scales may be affected by viscous effects. However, the largest scales generated by the shock wave might not be affected [54]. The initial condition is set at two computational regions: the one near the center of the cylinder is the source region and another is the ambient region. And the pressure and temperature in the source region are 12 MPa and 2000 K, respectively. The pressure and temperature in the ambient region are 0.1 MPa and 300 K, respectively. The computational mesh is a rectangular grid system with 10001×4001 grid points (x_{max} = 1000 $L_{1/2}$, y_{max} = 400 $L_{1/2}$) to reduce its numerical cost. The grid size in both the x and y direction is 4.6 μm (dx = dy = 0.1 $L_{1/2}$) and the boundary condition at the x and y axes are treated as symmetry and the upper and right sides of the boundary are treated as outlet. The gas in both regions is filled by a hydrogen-oxygen mixture.

5.0 RESULTS AND DISCUSION

The cylindrical detonation induced by direct initiation is simulated with different equivalence ratios in a hydrogen-oxygen mixture at the condition of P_0 = 1.0 atm and T_0 = 298.15 K. In the case that the half reaction length is wide, such as small equivalence ratios (ϕ = 0.2, 0.3) or large equivalence ratios (ϕ = 1.8, 2.0), the numerical simulation is stiff in the reaction term. At the case near the minimum half reaction length (see to Fig. 2), the direct numerical simulation of cylindrical detonation induced by the direct initiation can be performed two-dimensionally.

5.1 Cellular Structure

Figure 4 shows the maximum pressure histories at ϕ=0.4, 1.0, and 1.4. The pressure range is between 0.3 and 12.0 MPa. The dark and light area implies high and low pressure, respectively. The cellular pattern like the experimental smoked foiled record as shown in Fig. 5 is observed in the present numerical results in Fig. 4. The cellular structure denotes the trajectory of the transverse wave which propagates in a circumferential direction of detonation wave front. The ignition process at

stoichiometric ratio (ϕ=1.0) has two stages as shown by the cellular structure in Fig. 4 (b): the first stage is near the ignition source and the second stage starts at a certain distance from the ignition source. It is considered that the ignition processes at ϕ=0.4 and ϕ=1.4 are calculated just only for the first stage. As the first stage, the cells have unformed and complicate structure and become large with increasing the distance from the ignition source. At the second stage, numerous fine cells (cell bifurcations) appear due to generation of new transverse waves. This ignition process is experimentally observed by Edwards et al. [55] and Vasil'ev and Trotsyuk [56]. Figure 5 shows a smoked foil record [56] in a C_2H_2+2.5O_2 mixture. Although they obtained it in the different mixture from the one used in the present study, their cellular structure is similar to our numerical one (comparison of Fig. 4 and Fig. 5).

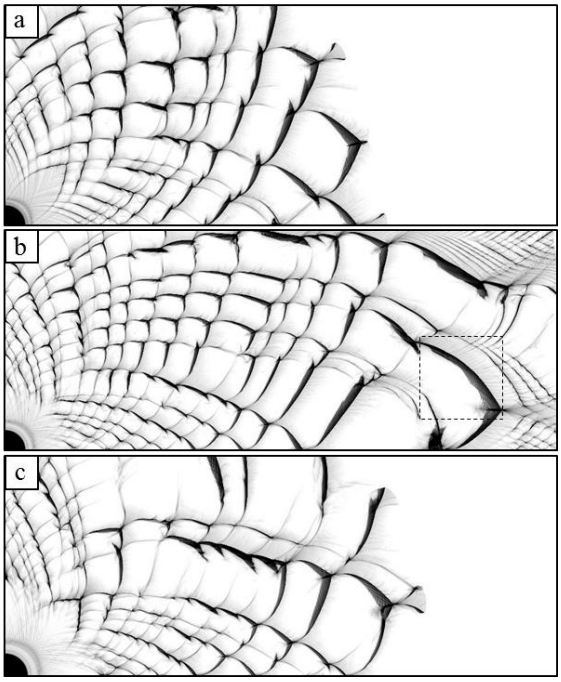

Figure 4. The maximum pressure histories of the cylindrical detonation induced by direct initiation in a hydrogen-oxygen mixture at ϕ=0.4, 1.0, 1.4. The pressure range is between 0.3 and 12.0 MPa. The dark area implies high pressure and the light area implies low pressure.

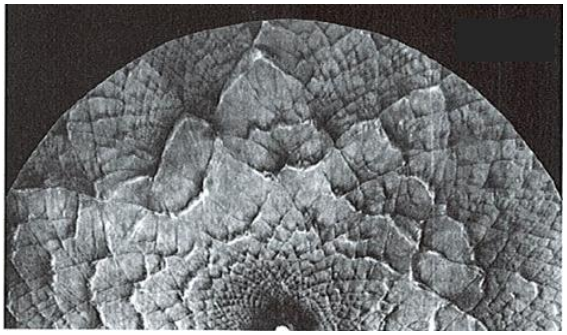

Figure 5. Experimental smoked foil record using a direct initiation at supercritical regime in a C_2H_2+2.5O_2 mixture [56].

5.2 Variation of Mean Cell Width

Figure 6a shows the relation between the distance from ignition source (the detonation front radius), *r*, and the mean cell width, λ, obtained by Vasil'ev and Trotsyuk [56] and Fig.6b shows the relation

between the distance from ignition source and the mean cell width calculated at the present simulation. The mean cell width, λ, is defined by

$$\lambda = \frac{2\theta r}{N_{TW}}, \tag{20}$$

where $N_{\mathrm{TW}}(r, \theta)$ – the number of transverse wave existing in the detonation front, θ – the angle of the arc where N_{TW} counts, rad. The experimental cell width becomes wide with increasing the distance form ignition source at the first stage and abruptly becomes constant at the second stage to the smaller size than the one just at the end of the first stage. The profile of the mean cell width in the numerical results is similar to the experimental one. The distance from ignition source and the mean cell width are normalized by the half reaction length, $L_{1/2}$. The normalized mean cell width, $\lambda/L_{1/2}$, at each equivalence ratio has a constant slope in Fig. 6b. Thus, the number of the transverse waves is nearly constant during propagating at the first stage, where the normalized cell width, $\lambda/L_{1/2}$, is independent of the equivalence ratio. Note that the normalized mean cell width, $\lambda/L_{1/2}$, corresponds to the proportional constant, A, defined as Eq. 19, which indicates that the phenomena defined by Eq. 19 should be also observed in the direct numerical simulations.

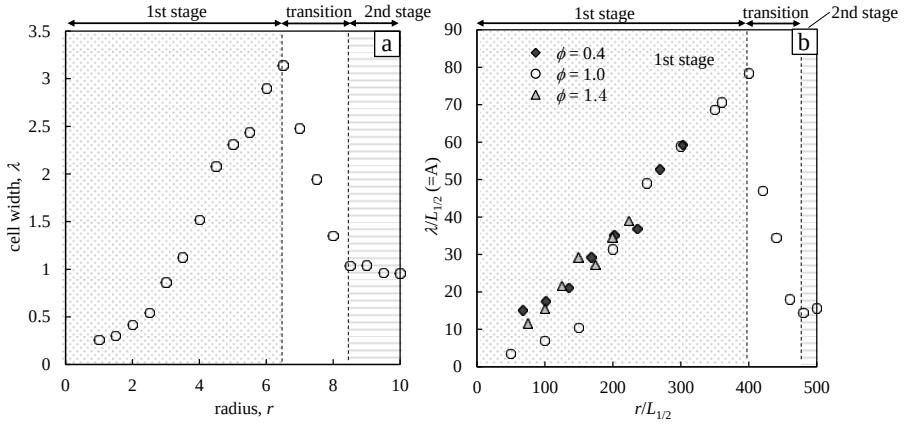

Figure 6. (a) The relation between the distance from source region and the experimental cell width in C_2H_2+2.5O_2 acetylene-oxygen mixture [56] and (b)the relation between the distance from source region and the numerical cell width in hydrogen-oxygen mixture obtained by the present simulations.

5.3 Cell bifurcation Mechanism

Transverse cells appear in the main cellular structure at the first stage near the second stage as shown by Fig. 4. Figure 7 shows the enlarged picture of transverse cells in the dashed square region in Fig. 4b. The transverse cell is small and unclear due to high pressure in the left upper region of Fig. 7 and becomes large and clear with propagating along the main cellular structure to the right bottom region of Fig. 7. The cellular boundary of A-side in Fig. 7 is sharp compared to that of B-side. Stamps et al. [57] and Vasil'ev and Trotsyuk [58] observed the similar cell pattern in a hydrogen-air detonation (they called it the subcellular structure). The transverse cell might have the same structure as the multi-headed ribbon observed by spinning detonation [59]. Gamezo et al. [60] and Mach and Radulescu [61] numerically obtained the transverse cell in two-dimensional detonation in a tube. They reported that the unsteadiness of marginal detonation produces the transverse cell. The instantaneous pressure contour and heat release contour in the square area-8 in Fig. 7 (just after the local explosion induced by the interference of transverse waves) are shown in Fig. 8 and those in the square area-9 of Fig. 7 (just before next local explosion) are shown in Fig. 9. The shock interaction with the detonation wave front is observed in the pressure contours in Fig. 8a and Fig. 9a. Figure 8 shows the double Mach reflection structure [62], where a Mach stem (a strong shock) interacts with an incident shock (a weak shock) to form a reflected shock, then these three shocks construct the primary triple point. The reflected shock and the transverse wave, which is formed by the pressure difference behind the Mach

stem and the incident shock, construct the secondary triple point. The chemical reaction is active behind the Mach stem and in the region between A and B near the transverse wave as shown in Fig 8b. Figure 9 shows the complex Mach reflection structure. Many secondary triple points and secondary transverse waves propagating upstream (the rightward in Fig. 9) and downstream (the leftward in Fig. 9) appear in the region between A and B, which is more extended than that in Fig. 8. The transverse wave with many secondary triple points, which is called the transverse detonation [60], traces the transverse cells. The secondary transverse wave to the upstream direction propagates across the primary triple point and interacts with the Mach stem. This interaction with the Mach stem might generate a new transverse wave. Thus, the transverse wave transforms to the transverse detonation as wide interproximal a space of transverse waves at the end of the first stage, and after that, the interaction generated by the secondary transverse wave at the Mach stem becomes the new transverse wave at the start of the second stage. The trajectory of the new transverse wave bifurcates the main cellular structure.

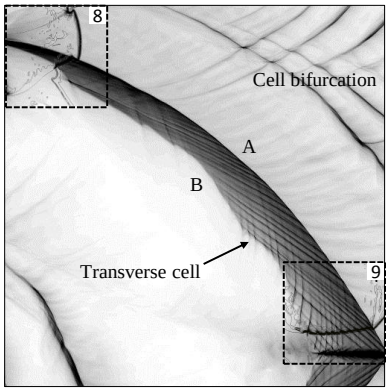

Figure 7. The enlargment view of the dashed square area in the maximum pressure history at ϕ=1.0 (Fig. 4b).

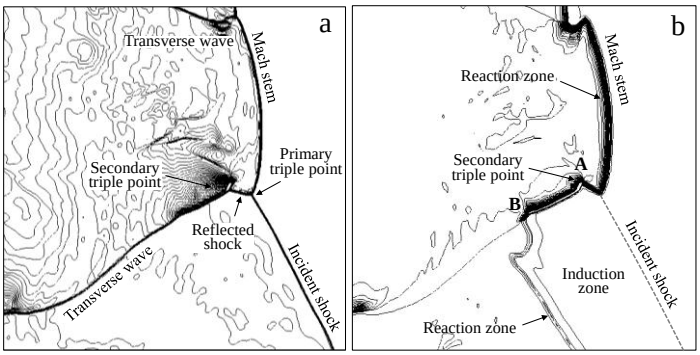

Figure 8. The instantaneous pressure contour and heat release contour in the square area-8 of Fig. 7.

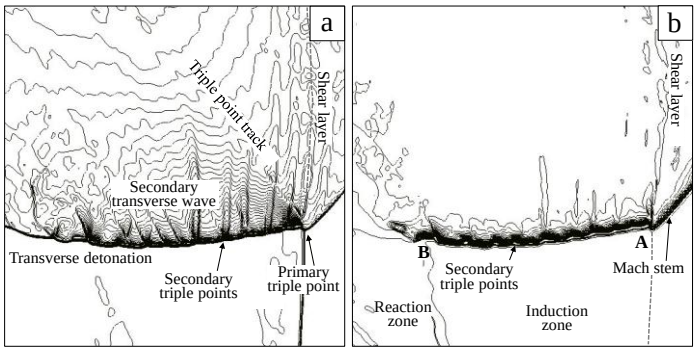

Figure 9. The instantaneous pressure contour and heat release contour in the square area-9 of Fig. 7.

6.0 CONCLUSIONS

The Chapman-Jouguet (CJ) values are calculated to understand the fandamental characteristics of hydrogen-oxygen mixture. In the numerical results of CJ detonation at the standerd state with different equivalence ratios of hydrogen-oxygen mixture, CJ pressure and CJ temperature draw the horseshoe-shape curve which have the local maximum value near the stoichiometric condition. CJ velocity increases grossly at the small equivalence ratios and does gently at the large equivalence ratios.

The equivalence ratio dependency with a detailed kinetic model is investigated that the half reaction length used by Notre Dame model is the longest among that by the others near the stoichiometric condition. However, compared the experimental cell width with the predicted one using by Pertersen-Hanson model provides the best agreement comparing with that of the others near the large equivalence ratio at the standard state.

The cylindrical detonation induced by direct initiation is simulated at several equivalence ratios in hydrogen-oxygen mixture. The cellular structure, which is similar to the experimental smoked foil record by Vasil'ev and Trotsyuk, is observed in the numerical simulation. The propagating process of cylindrical detonation induced by direct initiation has two stages. At the first stage, the cell width becomes wide with propagating. The normalized mean cell width, $\lambda/L_{1/2}$, at each equivalence ratio becomes increasing to constant slope. At the second stage, the cell width is constant due to the cell bifurcation. The transverse wave transforms to the transverse detonation with extending the transverse wave spacing at the end of the first stage, and after that, the disturbance generated by the secondary transverse wave at the Mach stem evolves to the new transverse wave at the start of the second stage. The trajectory of the new transverse wave bifurcates the main cellular structure.

ACKNOWLEDGMENTS

This research was supported by the JSS Systems in JAXA supercomputer system, the CMC in Osaka university supercomputer system and the research fellow of the Japan Society for the Promotion of Science, subject no. 21-9133.

REFERENCES

1. Investigation Report on Pipe Rupture Incident at Hamaoka Nuclear Power Station Unit-1, Nuclear and Industrial Safety Agency (NISA) and Ministry of Economy, Trade and Industry (METI), 2002.
2. Press release on condition of Fukushima Daiichi first nuclear power plant, http://www.tepco.co.jp/nu/f1-np/press_f1/2010/htmldata/bi1405-j.pdf
3. Urtiew, P.A. and Oppenheim, A.K., Experimental observation of the transition to detonation in an explosive gas, *Proc. Roy. Soc. London Ser*. **A 295**, 1966, pp. 13-28.
4. Liberman, M.A., Ivanov, M.F., Kiverin, A.D., Kuznetsov, M.S., Rakhimova, T.V. and Chukalovskii, A.A., On the Mechanism of the Deflagration-to-Detonation Transition in a Hydrogen-Oxygen Mixture, *J. Experimetal and Theoretical physics*, **111**, 2010, pp. 684-698.
5. Liberman, M.A., Ivanov, M.F., Kiverin, A.D., Kuznetsov, M.S., Chukalovsky, A.A. and Rakhimova, T.V., Deflagration-to-detonation transition in highly reactive combustible mixtures, *Acta Astronautica*, **67**, 2010, pp. 688-701.
6. Zel'dovich, Y.B., Kogarko, S.M. and Simonov, N.N., An Experimental Investigation of Spherical Detonation in Gases, *Sov. Phys. Tech. Phys.*, **1**, 1956, pp. 1689-1713.
7. Bach, G.G., Knystautas, R. and Lee, J.H., Direct Initiation of Spherical Detonation in Gaseous Mixtures, *12th Int. Symp. Combust.*, 1969, pp. 853-864.
8. Bach, G.G., Knystautas, R. and Lee, J.H., Initiation Criteria for Diverging Gaseous Detonations, *13th Int. Symp. Combust.*, 1970, pp. 1097-1110.
9. Lee, J.S.H., Initiation of Gaseous Detonation, *Ann. Rev. Phys. Chem.*, **28**, 1977, pp. 75-104.
10. Edwards, D.H., Hooper, G., Morgan, J.M. and Thomas, G.O., The Quasi-steady Regime in Critically Initiated Detonation Waves, *J. Phys. D.*, **11**, 1978, pp853-864.

11. Lee, J.H. and Ramamurthi, K., On the Concept of the Critical Size of a Detonation Kernel, *Combust. Flame*, **7**, 1976, pp. 331-340.
12. Lee, J.H. and Matsui, H., A Comparison of the Critical Energies for Direct Initiation of Spherical Detonations in Acetylene-Oxygen Mixtures, *Combust. Flame*, **28**, 1977, pp. 61-66.
13. Lee, J.H.S., Dynamic Parameter of Gaseous Detonations, *Ann. Rev. Fluid Mech.*, **3**, 1984, pp. 311-336.
14. Benedick, W.B., Guirao, C.M., Knystautas, R. and Lee, J.H.S., Critical charge for the direct initiation of detonation in gaseous fuel-air mixtures, *Prog. Astronaut. Aeronaut*, **106**, 1986, pp. 181-202.
15. Matsui, H. and Lee, J.H., On the measure of the relative detonation hazards of gaseous fuel-oxygen and air mixtures, 17th Symp. (Int.) on Combustion, 1978, pp. 1269-1280.
16. He, L. and Clavin, P., On the direct initiation of gaseous detonations by an energy source, *J. Fluid Mech.*, 1994, pp. 227-248.
17. He, L., Theoretical Determination of the Critical Conditions for the Direct Initiation of Detonations in Hydrogen-Oxygen Mixtures, *Combust. Flame*, **104**, 1996, pp. 401-418.
18. Eckett, C.A., Quirk, J.J. and Shepherd, J.E., The role of unsteadiness in direct initiation of gaseous detonations, *J. Fluid Mech.*, **421**, 2000, pp. 147-183.
19. Ng, H.D. and Lee, J.H.S., Direct initiation of detonation with a multi-step reaction scheme, *J. Fluid Mech.*, **476**, 2003, pp. 179-211.
20. Ng, H.D., Ju, Y. and Lee, J.H.S., Assessment of detonation hazards in high-pressure hydrogen storage from chemical sensitivity analysis, *Int. J. Hydrogen Energy*, **32**, 2007, pp. 93-99.
21. Ng. H.D. and Lee. J.H., Comments on explosion problems for hydrogen safety, *J. Loss Prevent. Process Ind.*, **21**, 2008, pp. 136-146.
22. Watt, S.D. and Sharpe, G.J., Linear and nonlinear dynamics of cylindrically and spherically expanding detonation waves, *J. Fluid Mech.*, **522**, 2005, pp. 329-356.
23. Nirasawa, T. and Matsuo, A., Multidimensional Wave Propagation of Direct Initiation on Detonation, *21th ICDERS*, 2007.
24. Asahara, M., Tsuboi, N., Hayashi, A.K. and Yamada, E., Two-Dimensional Simulation on Propagation Mechanism of H2/O2 Cylindrical Detonation with Detailed Reaction Model: Influence of Initial Energy and Propagation Mechanism, *Combust. Sci. Tech.*, **182**, 2010, pp. 1884-1900.
25. Jiang, Z., Han, G., Wang, C. and Zhang, F., Self-organized generation of transverse waves in diverging cylindrical detonations, *Combust. Flame*, **156**, 2009, pp. 1653-1661.
26. Tanaka, K., AISTJAN, http://www.aist.go.jp/RIODB/ChemTherm/gas.html
27. Stull, D. and Prophet, H., JANAF thermochemical tables, 2nd ed. NSRDS-NBS37, 1971.
28. Hishida, M., and Hayashi, A.K., Numerical Simulation of Pulsed Jet Plume Combustion, *13th ICDERS*, 1991.
29. Petersen, E.L. and Hanson, R.K., Reduced Kinetics Mechanisms for Ram Accelerator Combustion, *J. Prop. Power*, **15**, 1999, pp. 591-600.
30. Li, J., Zhao, Z., Kazakov, A. and Dryer, F.L., An Updated Comprehensive Kinetic Model of Hydrogen Combustion, *Int. J. Chem. Kinet.*, **36**, 2004, pp. 566-575.
31. O'Conaire, M., Curran, H.J., Simmie, J.M., Pitz, W.J. and Westbrook, C.K., A Comprehensive Modeling Study of Hydrogen Oxidation, *Int. J. Chem. Kinet.*, **36**, 2004, pp. 603-622.
32. Powers, J.M. and Paolucci, S., Accurate Spatial Resolution Estimates for Reactive Supersonic Flow with Detailed Chemistry, *AIAA J.*, **43**, No. 5, 2005, pp. 1088-1099.
33. Konnov, A.A., Remaining uncertainties in the kinetic mechanism of hydrogen combustion, *Combust. Flame*, **152**, 2008, pp. 507-528.
34. Shimiz, K., Hibi, A., Koshi, M., Morii, Y. and Tsuboi, N., An Updated Kinetic Mechanism for High-Pressure Hydrogen Combustion, *J. Prop. Power*, **27**, No. 2, 2011
35. Barthel, O.H., Predicted Spacings in Hydrogen-Oxygen-Argon Detonations, *Phys. Fluids*, **17**, 1974, pp. 1547-1553.
36. Tsuboi, N., Asahara, M., Eto, K. and Hayashi, A.K., Numerical simulation of spinning detonation in square tube, *Shock Waves*, **18**, 2008, pp. 329-344.
37. Tsuboi, N., Asahara, M. and Hayashi, A.K., Effect of initial pressure on spinning detonation in a

square tube, *Sci. Tech. Energetic Materials*, **69**, 2008, pp. 173-176.
38. Burke, M.P., Chaos, M., Dryer, F.L. and Ju, Y., Non-monotonic Pressure Dependence in Laminar Mass Burning Rates for Hydrogen Flames, *AIAA paper*, 2009, 09-990.
39. Tsuboi, N., Asahara, M., Hayashi, A.K. and Koshi, M., Effects of detailed chemical reaction model on detonation simulations, *Shock Waves*, **4**, 2009, pp. 233-238.
40. Adachi, S. Hayashi, A.K., Morii, Y., Tsuboi, N., and Yamada, E., Effects of Chemical Reaction Model on H_2/O_2 Detonation at High Pressures, *AIAA paper*, 2009, 09-0441.
41. Strohle, J. and Myhrvold, T., An evaluation of detailed reaction mechanisms for hydrogen combustion under gas turbine conditions, *Hydrogen Energy*, **32**, 2007, pp. 125-135.
42. Shchelkin, K.I. and Troshin. Y.K., Gasdynamics of combustion, Mono Book Corp., 1963
43. Knystautas, R., Guirao, C., Lee, J.H. and Sulmitras, A., Measurement of cell size in hydrocarbon-air mixtures and prediction of critical tube diameter, critical initial energy and detonability limits, *Prog. Astronaut. Aeronaut*, **94**, 1984, pp. 23-37.
44. Westbrook, C.K., Hydrogen oxidation kinetics in gaseous detonations, *Combust. Sci. Tech.*, **29**, 1982, pp. 67-81.
45. Bull, D.C., Elsworht, J.E. and Shuff, P.J., Detonation Cell Structures in Fuel/Air Mixtures, *Combust. Flame*, **45**, 1982, pp. 7-22.
46. Sheperd, J.E., Chemical kinetics of hydrogen-air-diluent detonations, *Prog. III Astro. Aero.*, **106**, 1984, pp. 263-293.
47. Stamps, D.W., Slezak, S.E., Tieszen, S.R., Observations of the cellular structure of fuel-air detonations, *Combst. Flame*, **144**, 2006, pp. 289-198.
48. Sussman, M.A., Computational Study of Unsteady Shock Induced Combustion of Hydrogen-air mixtures, *AIAA Paper*, 1994, 94-3101.
49. Shepherd, ZND, http://www.galcit.caltech.edu/EDL/public/32bitChemkinPC/znd/
50. Ohyagi, S., Ochiai, T., Yoshihashi, T. and Harigaya, Y., Relation between Cell Size, Induction Zone Length and Critical Initiation Energy in Oxyhydrogen Detonations, *Trans. Jpn. Soc. Mech. Eng.* B 54, **54**, No. 508, 1988, pp.3559-3564.
51. Wada, Y. and Liou, M., A Flux Splitting Scheme with High Resolution and Robustness for Discontinuities, *AIAA Paper*, 1994, 94-0083.
52. Liou, M.S., On a Class of Neew Flux Splitting Schemes, *Lecture Notes in Physics*, **414**, 1992, pp.115-119.
53. Shuen, J.S., Upwind Differencing and LU Factorization for Chemical Non Equilibrium Navier-Stokes Equations, *J. Comput. Phys.*, **99**, 1992, pp. 233-250.
54. Oran, E.S., Weber Jr., J.W., Lefebvre, M.H. and Anderson Jr., J.D., *Combust. Flame*, **113**, 1998, pp. 147-163.
55. Edwards, D.H., Hooper, G., Morgan, J.M. and Thomas, G.O., The Quasi-steady Regime in Critically Initiated Detonation Waves, *J. Phys. D.*, **11**, 1978, pp853-864.
56. Vasil'ev, A.A. and Trotsyuk A.V., Experimental Investigation and Numerical Simulation of an Expanding Multifront Detonation Wave, *Combust. Explo. Shock waves*, **39**, 2003, pp. 80-90.
57. Stamps, D.W., Slezak, S.E. and Tieszen, S.R., Observations of the cellular structure of fuel-air detonations, *Combust. Flame*, **144**, 2006, pp. 289-298.
58. Vasil'ev, A.A., Vasiliev, V.A. and Trotsyuk A.V., Bifurcation structures in gas detonation, *Combust. Expo. Shock Waves*, **46**, No. 2, 2010, pp.196-206.
59. Lee, J.H., Soloukin, R.I. and Oppenheim, A.K., Current Views on Gaseous Detonation, Astronaut. Acta., **14**, 1969, pp. 565-584.
60. Gamezo, V.N., Vasil'ev, A.A., Khokhlov, A.M. and Oran, E.S., Fine Cellular Structures Produced by Marginal Detonations, *Int. Symp. Combust.*, **28**, 2000, pp. 611-617.
61. Mach, P. and Radulescu, M.I., Mach reflection bifurcations as a mechanism of cell multiplication in gaseous detonations, *Proc. Combust. Int.*, **33**, 2011, pp.2279-2285.
62. Inaba, K., Matsuo, A. and Tanaka, K., Numerical Investigation on Acoustic Coupling of Transverse Waves in Two-Dimensional H2-O2-Diluent Detonations, Trans. Japan Soc. Aero. Space Sci., **47**, No. 158, 2005, pp 249-255.